Evaluation of Deformation Behavior of Self-Standing Retaining Wall Using Large Diameter Steel Pipe Piles into Hard Ground

Yoshiro ISHIHAMA
Senior Researcher, Steel Structures Research Lab., Nippon Steel and Sumitomo metal Corporation, Chiba, Japan
Email: ishihama.86m.yoshiro@jp.nssmc.com
Kakuta FUJIWARA
Manager, Construction Products Development Div., Nippon Steel and Sumitomo metal Corporation, Tokyo, Japan
Jiro TAKEMURA
Associate Professor, School of Environment and Society Department of Civil and Environment Engineering, Tokyo Institute of Technology, Tokyo, Japan
V. KUNASEGARAM
Student, School of Environment and Society Department of Civil and Environment Engineering, Tokyo Institute of Technology, Tokyo, Japan

ABSTRACT

Steel pipe pile walls are utilized for many projects. Recently, the application of the walls has increased especially for high walls. In such a case, the pile diameter should be larger in order to gain high flexural rigidity and the embedded ground should be stiff enough to satisfy the requirement for the wall displacement. A conventional method such as Chang's formula has been used in the design of such high walls, but several difficulties in design and construction are arising due to the natures of larger diameter pile. With respect to the design issues, the embedment of the walls determined by the conventional method becomes longer beyond necessity for stability, since the higher flexural rigidity of larger diameter of piles is one of the critical conditions for the minimum embedment depth. In case of harder ground conditions, the longer embedment is likely to lead to difficulties in installing piles and hereby causes extra construction time and cost. In this paper the behavior of wall with large-diameter steel pipe piles embedded into a soft rock is investigated by a simple analysis using a beam-spring model targeting the wall embedment length as the main parameter. The calculated results were compared with those observed in centrifuge models. The results of this study suggest that the conventional method could require unnecessary embedment length and then the calculation model with Elasto-Plastic soil springs can determine more rational embedment length even if the larger diameter piles are used for retaining walls into stiff layers.

Key words: *Steel pipe pile, Retaining wall, Soft rock, Frame model analysis, Centrifuge*

1. Introduction

Construction projects aiming to make efficient use of small plots of land and mountainside road projects have increased in recent years, necessitates the use of tall self-standing steel pipe retaining walls. As the height of retaining wall increases, the need is growing for high-flexural-rigidity steel pipes in order to achieve wall top displacement reduction, which is a critical structural performance requirement. Consequently, the diameter of steel pipes used for such applications becomes larger. The embedment length of a steel pipe in the ground is determined by the larger one between the minimum required embedment length and calculated length satisfying the required wall deformation, such as wall top displacement. The minimum depth is determined by a conventional method, such as Chang's method, using a

formula of the steel pipe flexural rigidity and ground rigidity. If, however, a large-diameter (e.g. greater than 2,000 mm) steel pipe is used, there are cases where the required embedment length becomes very large, even for the hard ground, because high steel pipe flexural rigidity makes the minimum required embedment length by Chang's or other method so large. For example, 2,000 mm diameter piles require embedment length over 10 m even in the ground consisting of sand and gravel layers with SPT N-value greater than 50, regardless of the wall height. Such large embedment depth would place a very heavy burden on the constructor. The authors conducted a series of centrifuge tests focusing mainly on embedment in soft rock (Kunasegaram *et al*., 2018) and confirmed that stability requirements could be met even if a substantially shorter embedment length (about 1/2 to 1/3) compared to the minimum length determined by the conventional design method. When evaluating the behavior of a retaining wall with a shorter embedment length by using a calculation model, it is necessary to evaluate ground behavior including the transition from the elastic range to the plastic range in the embedment zone, and such behavior cannot be evaluated by applying the beam-on-elastic-foundation theory. In this study, therefore, the validity of applying the Elasto-Plastic design method to a retaining wall with a short embedment length was verified by comparing calculation results based on the Elasto-Plastic design method with the centrifuge test results. Furthermore parametric study was made on the embedment length in the calculation.

2. Calculation model of Elasto–Plastic method

In accordance with JASPP's design manual (JASPP 2008), the calculation model shown in **Fig. 1** and the calculation conditions shown in **Table 1** were defined. The retaining wall was modeled as an elastic beam element whose lower end is connected to a pin-roller support. The reason why the elastic beam element was used is that under the calculation conditions assumed, the member stresses in all cases were within the elastic range.

For the embedment zone, a bi-linear elastic and perfectly plastic soil spring as shown in **Fig. 2** was defined. The setup for the centrifuge test (Kunasegaram *et al*., 2018) conducted for comparison is shown in Fig. 3.

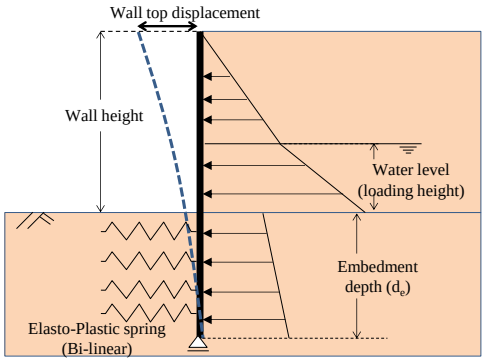

Fig. 1 Calculation model of Elasto–Plastic design method

Table 1. Calculation and experimental conditions

Case name	C2	C3	C4	C7
Wall thickness (=pile diameter) (m)	1.0	2.5	2.5	2.5
Wall height (m)	9.0	12.0	12.0	12.0
Embedment depth (d_e) (m)	1.8	9.8	3.0	2.5
Embedment requirement by Chang's method (d_c) (m)	6.4	16.3	11.2	11.2
Ratio of d_e to d_c	28%	60%	27%	22%
k_H (MPa)	150	56	250	250
Upper limit of subgrade reaction coefficient (MPa)*	1.1	0.07	1.4	1.4
Calculation Water level (m) (=Loading height)	0→6.0	0→7.0	0→8.03	0→9.8

*: Rankine passive pressure determined by q_u (unconfined compressive strength) for soft rock and ϕ' for sand.

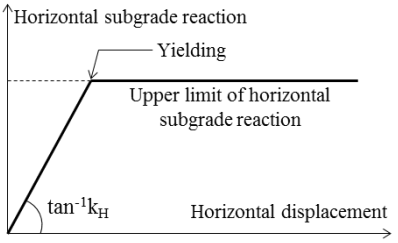

Fig. 2 Horizontal subgrade reaction model

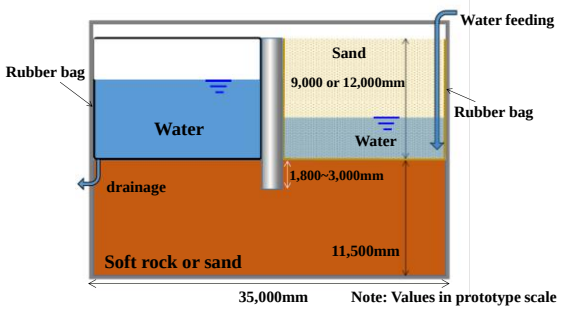

Fig. 3 Experimental setup in centrifuge

A sealed rubber bag containing water was placed in front of an aluminum wall secured to the embedment zone,

and an open-top rubber bag containing dry Toyoura sand was placed at the back of the wall. The test was conducted in two stages: excavation and loading. At the excavation stage, the water in the rubber bag in front of the wall was drained into a tank to let the pressure from the dry sand act on the wall. At the loading stage, the water in the tank was poured into the rubber bag at the back of the wall so that the water level rose gradually so as to increase the load acting on the wall. Thus, the process leading to the ultimate state was examined by observing the deformation behavior of the retaining wall.

The properties of the soft rock and sand used were determined with reference to unconfined compressive test results and past experiment results (Koda *et al.*, 2000), respectively. In the calculation, attention was paid to the water level, and the load condition at the end of the loading (water level = 0 m; hereinafter referred to as "loading height") was defined as the initial condition. Thereafter, retaining wall deformation taking place in response to the loading height rise was calculated by the Elasto-Plastic design method, and the results thus obtained were compared to the centrifuge test results. The load acting from behind the wall was assumed to consist of water pressure and earth pressure. The earth pressure was calculated by assuming an internal friction angle, φ, of 40°, a cohesion, c, of 0 kN/m^2 and a coefficient of Rankin active earth pressure, K_a, of 0.215. In Case C3, a horizontal load corresponding to the overburden load was also applied because the embedment layer is composed of sand. For comparison, **Fig. 4** shows the horizontal load ratio and the moment ratio at each loading height. Horizontal load ratio and the moment ratio are the relative values to the water level of 0 m. As shown, the horizontal load increases more gently than the moment as the loading height increases. The flexural rigidity of the wall and the embedment length used in the test were determined in advance through the preliminary design so that the wall top displacement at a loading height of 0 m would not exceed 50 mm, which is the limit under normal conditions used in the design of river structures such as revetments. However, in this calculation and experiment, it is not considered that the limit of the minimum embedment length was determined from the characteristic value by Chang's formula.

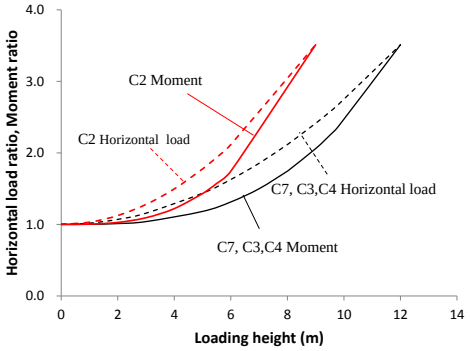

Fig. 4 Moment and horizontal load with loading height

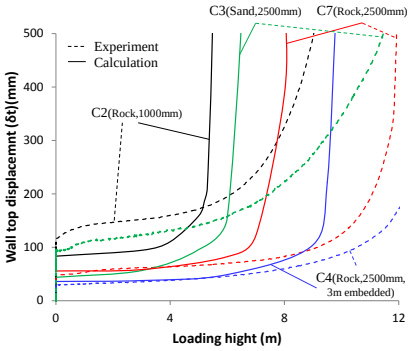

Fig. 5 Relationship between wall top displacement and loading height

3. Calculation result and discussions

3.1. Yielding and influence of embedment depth

Fig. 5 compares the calculated and measured values showing the relationship between loading height and wall top displacement. Case C2 and Case C3 show slight differences in initial displacement at the start of loading (loading height = 0 m; upon completion of excavation in front of the wall). This is thought to be because in C3 rigidity was assumed to be constant in the depth direction, while in the test rigidity varied in the depth direction. In all cases in the centrifuge test, displacement increased as the loading height rose, but the changes in displacement were gentler than in the calculation results. In contrast, in the calculation results, displacement began to increase sharply at a particular loading height (5.0 m in C2, 5.8 m in C3, 9.6 m in C4, 6.8 m in C7) showing a clear infection point. The reason for this is that because the soil spring at the embedment zone is modeled as a bi-linear elastic and perfectly plastic element as a condition for calculation (**Fig. 2**). Deformation continues to increase even after the yielding without increase of the horizontal resistance. It is thought that in the test, passive resistance increased, regardless of the type of ground (soft rock or sand), as ground deformation in the

embedment zone could increase after the yielding. From these results, it can be inferred that calculation by the Elasto-Plastic design method could make it possible to estimate deformation behavior conservatively until the point of inflection was reached. The load at the loading height at the point of inflection was greater than the design load under normal conditions (at a loading height of 0 m) by a factor of about 1.6 to 1.8 in the horizontal direction, and the moment was greater than the design value by a factor of about 1.3 to 1.5.

3.2. Bending moment – deflection and failure

Fig. 6 shows bending moment distributions per unit width in the retaining wall. Although the calculation and test results show fair agreement in tendency, in all cases the measured bending moment tended to be greater than the calculated moments at loading heights from 0.0 to 3.0 m. Thereafter, the calculated and measured values of bending moment were more or less the same or the calculated values were greater than the measured values. In the calculation, Rankin active condition was assumed on the earth pressure acting on the wall from the backfilled sand from the beginning of the loading. But the actual wall earth pressure after the excavation process might not reach the active condition and additional load was needed to get the active condition. This could be a possible reason of overestimation of bending moment in the beginning of loading and better agreement between the calculations and measurements.

In the cases where the ground in the embedment zone consists of soft rock (C2, C4 and C7), the maximum bending moment occurred in the region just under the surface of the embedment zone. Both test and calculation results indicate that the retaining wall is firmly confined by soft rock with very high rigidity (See Table 1). In contrast, in the case where the embedment zone consists of sand (C3), as loading height increased, the location where the maximum bending moment occurred became gradually deeper. **Table 2** shows the location of the pivot point of rotation. In the centrifuge tests of soft rock ground, the measured pivot points of rotation were located slightly below the midpoint of the embedment length. In the sand cases with relatively deep embedment, the pivot point of rotation was located close to the lower end of the embedded wall. The calculation results indicate that the pivot point of rotation is located at a depth corresponding to 56% to 57% of the embedment depth in the soft rock cases and at a depth corresponding to about 80% of the embedment depth in the sand case. These calculation results agree fairly well with the test results.

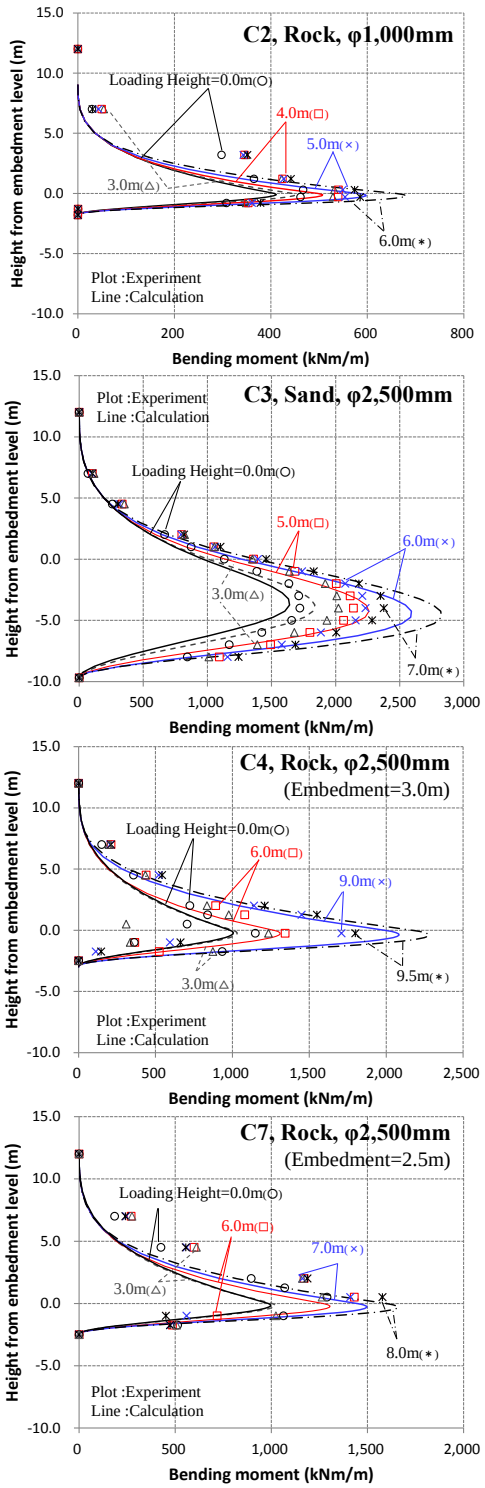

Fig. 6 Bending moment profiles at the loading

Table 2. Pivot points of rotation at failure

		Pivot point (d_p) from embedment level (m)	Embedment length (d_e) (m)	d_p/d_e
C2	Cal	1.01	1.8	0.561
	Exp	1.05		0.581
C3	Cal	7.70	9.8	0.786
	Exp	6.80		0.694
C4	Cal	1.70	3.0	0.567
	Exp	1.56		0.521
C7	Cal	1.42	2.5	0.568
	Exp	1.28		0.510

3.3. Plastic area development in the embedment

Fig. 7 show how the plastic region increases with loading height. Here the plastic region is defined as the depth at which the horizontal sub-grade reaction reaches the upper limit (See **Table 1**). The plasticization ratios, defined by ratio of the thickness of plastic region to the embedment depth, are plotted to the loading height in Fig.8. In Case C2 with smaller equivalent pile diameter (φ1,000 mm), the plasticization occurs in the shallower region, while in Cases C4 and C7 with larger pile diameter (φ2,500 mm), the plasticization occurs more or less uniformly in the shallow and deep depth in the embedment zone. In Case C3, as can be seen, the plasticization begins and occurs to a considerable extent in the shallow region until loading height reach 6.0 m at the stage close to the ultimate state, when the plasticization begins near the lower end of the pile. Comparison of the calculation results on Cases C2, C4 and C7 (soft rock cases) with that of Case C3 (sand case) reveals that in the soft rock cases the plasticization occurs rapidly, while in the sand case the plasticization begins and occurs gradually from the shallow depth until the ultimate state was reached soon after the plasticization develops near the lower end of the pile. This is thought to be closely connected to the fact that in the soft rock, the pivot point of rotation was shallow and located near the midpoint of the embedment depth as shown in Section 3.2.

3.4. Horizontal subgrade reaction

Fig. 9 shows the effect of embedment on the wall top displacement calculated for the conditions of Case 2, 3 and 7 (**Table 3**). For the conditions of Cases C3 and C7 the displacement increases sharply as the embedment

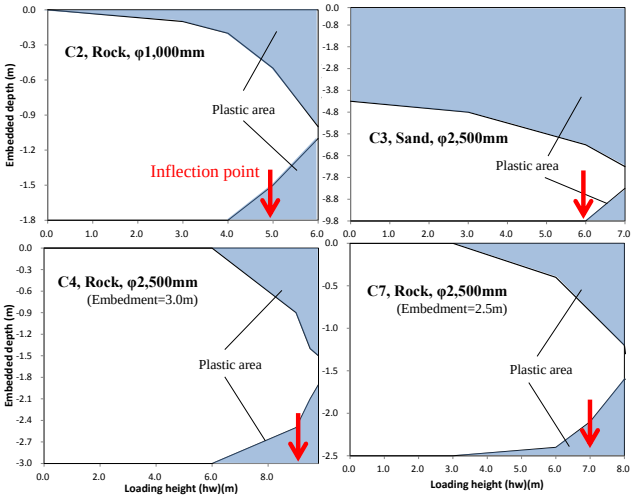

Fig. 7 Development of plastic region in the embedded depth with loading

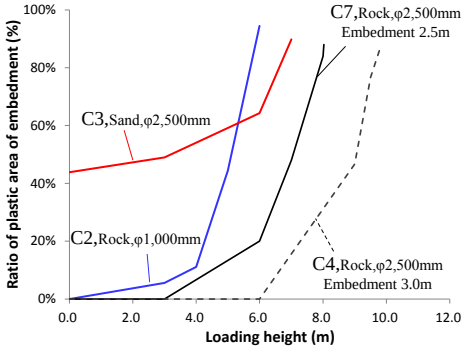

Fig. 8 Ratio of plastic area of embedment

Table 3. Calculation condition changing embedment

Calculation Case	C2'	C3'	C7'
Wall thickness (m)	1.0	2.5	2.5
Wall height (m)	9.0	12.0	12.0
Embedment (m) (Experiment→Calculation)	**1.8→ 1.3~6.0**	**9.7→ 8.3~18.0**	**2.5→ 1.8~8.0**
k_H (MPa)	150	56	250
Upper limit of subgrade reaction coefficient (MPa)	1.1	0.07	1.4
Loading height (m)	0.0	0.0	0.0

length is reduced by about 1 m from the length used in the experiment, while for the conditions of Case 2 a sharp increase only 0.3 m embedment depth reduction.

Fig. 10 shows the relationship between the embedment ratio and the amount of wall top displacement. The embedment ratio is relative value to the tested embedment length in Cases C2, C3 and C7. Fig. 11 shows the relationship between the embedment ratios relative to embedment requirement based on

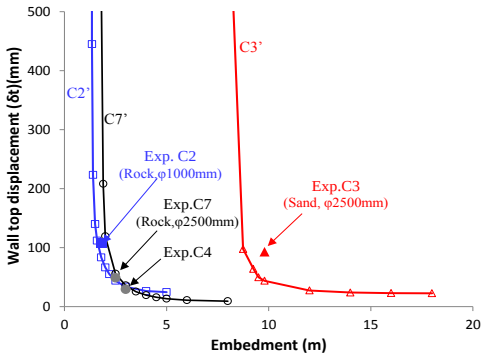

Fig. 9 Relationship between wall top displacement and embedment

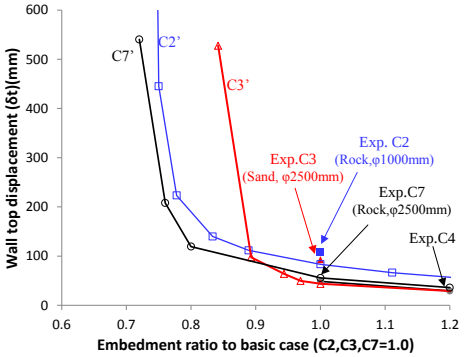

Fig. 10 Relationship between wall top displacement and embedment ratio

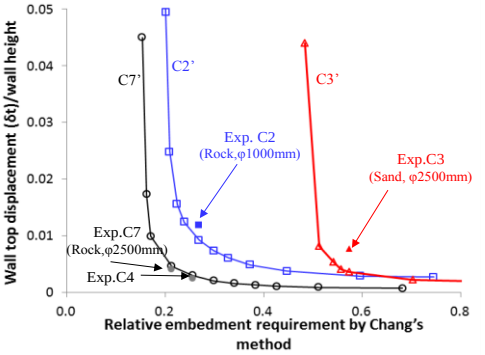

Fig. 11 Relationship between wall top displacement and relative embedment to the required one by conventional method

Chang's method and normalized wall top displacement by the wall height.

As shown in **Fig. 10**, in Case C3 (embedded in sand), the displacement begins to increase sharply when the embedment ratio decreases by about 10%. In Cases C7 and C2, the displacement begins to increase after the embedment ratio decreases by about 20% to 25%. From the results on the soft rock (i.e. hard ground) cases shown in Fig.11, it can be confirmed that no significant change in the wall displacement is obtained over a certain embedment. This embedment can be considered as a critical depth, over which wall behaves similar to the one with semi-infinite length. These critical lengths are about 30% to 40% of the embedment length required by the conventional method. In the sand case, however, the critical embedment length is about 60% to 70% the required embedment length. This indicates that the minimum embedment length requirement by the conventional method based on Chan's formula could be an over conservative in the assessment of wall displacement for the large diameter steel pipe wall constructed in the stiff ground, like soft rock.

4. Concluding remarks

・The plasticized length of embedment calculated by the Elasto-Plastic design method using a soil spring of a bi-linear elastic and perfect plastic element is not more than 50% under a horizontal load and a moment load greater than those assumed in design for normal load conditions by a factor of up to about 1.6 to 1.8 and by a factor of up to about 1.3 to 1.5, respectively. If applied loads are within those ranges, retaining wall behavior can be evaluated by the Elasto-Plastic design method.

・Under larger loads, the amount of displacement tends to be overestimated (i.e. to be on the safe side). In order to enhance the accuracy of retaining wall behavior estimation, it is necessary to refine the modeling approach by, for example, expressing ground behavior with a tri-linear model instead of a bi-linear model.

5. Acknowledgements

The authors gratefully acknowledge the invaluable advice and guidance provided by the members and advisers of the IPA TC1 (Committee on Application of Self-retaining Tubular Pile Wall to Stiff Ground) in connection with the preparation of this paper.

References

Kunasegaram, V. et al. 2018. Behavior of self-standing high stiffness steel pipe sheet pile walls embedded in soft rocks. Proceeding of the 1st International Conference on Press-in Engineering.

Japanese Association for Steel Pipe Piles. 2008. Deign manual of self-standing steel sheet pile wall. Try, co. ltd. (in Japanese)

Koda, M. et al. 2000. Modeling and evaluation of p-y curves of single pile in sand. Journal of Japan Society of Civil Engineers, pp. 191-207.